High-spin $(f_{7/2})^{A-40}$ states in ^{47}Ti, ^{47}Sc, ^{44}Ca, ^{45}Ca, and ^{48}Ti via ^{36}S + ^{14}C fusion-evaporation reactions

E. K. Warburton
Department of Physics, Brookhaven National Laboratory, Upton, New York 11973

C. W. Beausang, D. B. Fossan, L. Hildingsson, and W. F. Piel, Jr.
Department of Physics, State University of New York at Stony Brook, Stony Brook, New York 11794

J. A. Becker
Lawrence Livermore National Laboratory, Livermore, California 94550
(Received 28 January 1986)

^{36}S(^{14}C,$xnypz\alpha\gamma$) reactions were used to extend our knowledge of the high-spin states of ^{47}Ti, ^{47}Sc, ^{44}Ca, ^{45}Ca, and ^{48}Ti. The decay schemes were constructed from $\gamma\gamma$-coincidence data and γ-ray angular distributions and excitation functions. The angular distributions also provided information on spin-parity assignments and multipole mixing ratios. Lifetime information was extracted from analysis of the γ-ray Doppler shifts observed in both the angular distribution and $\gamma\gamma$-coincidence data. Assuming the probable J^π assignments are correct, the yrast schemes for all five nuclei extend to the highest spin allowed for $(f_{7/2})^{A-40}$. Results are compared to shell-model predictions generated in three different configuration spaces: $(f_{7/2})$, $(d_{3/2},f_{7/2})$, and the full (f,p) shell.

I. INTRODUCTION

In the mass region where the first $f_{7/2}$ shell is being filled by both protons and neutrons the yrast and near-yrast states appear to be largely explained by shell-model calculations[1,2] involving the $(f_{7/2})^n$ configurational space alone.[3] It thus appears that in the middle of the shell the possibility exists for testing our knowledge of nuclear structure to quite high excitations and angular momentum with a comparatively simple model. Indeed, such a comparison has been made for ^{48}Ti by Glatz *et al.*[4] who studied the high-spin states of ^{48}Ti via the ^{45}Sc(α,pγ)^{48}Ti reaction. They populated even-parity states up to a (very) probable J^π of 12^+ at an excitation energy of 8091 keV and made a detailed comparison of their results to the $(f_{7/2})^8$ predictions of Kutschera, Brown, and Ogawa.[2] A spin of 12 is the highest allowed by a simple $f_{7/2}$ model in ^{48}Ti. By contrast, previous experiments on ^{47}Ti have populated states only up to a known $\frac{19}{2}^-$ state at 4494 keV (and a possible $\frac{21}{2}^-$ state at 5197 keV), whereas the $(f_{7/2})^n$ model allows a high-spin state of $\frac{27}{2}^-$ at $\sim$8.6-MeV excitation. The present study was undertaken in order to extend our knowledge of yrast states in ^{47}Ti to higher spin and excitation. At the same time similar information was also obtained for ^{47}Sc, ^{44}Ca, ^{45}Ca, and ^{48}Ti.

As reviewed in the lastest compilation,[5] previous studies which extended our knowledge of high-spin states in ^{47}Ti include the ^{44}Ca(α,nγ)^{47}Ti work of Sawa, Blomqvist, and Guillholmer;[6] the ^{45}Sc(α,npγ)^{47}Ti study of Meyer-Schützmeister, Hardie, and Sjoreen;[7] and the ^{44}Ca(^{7}Li,p3nγ)^{47}Ti results of Fortuna, Lunardi, Morando, and Singorini.[8] Our study utilizes the ^{36}S(^{14}C,3nγ)^{47}Ti reaction. A fusion-evaporation reaction with $A=14$ and 36 is the most symmetric (i.e., most nearly equal masses of target and projectile) that one can use to form ^{47}Ti with a three-nucleon emission channel. As such, it constitutes the most nearly ideal reaction for forming high spins in ^{47}Ti. It also forms ^{47}Ti with a good signal to background ratio. This point is illustrated in Table I which compares fusion-evaporation calculations using CASCADE (Ref. 9) with the observed population of nuclei in the present study.

As summarized in Table I, the nuclei ^{47}Sc, ^{44}Ca, ^{45}Ca, and ^{48}Ti were all formed with cross sections about an order of magnitude less than that of ^{47}Ti. Nevertheless, new information was also obtained on the yrast schemes of ^{47}Sc and ^{45}Ca, as well as information on ^{44}Ca and ^{48}Ti which corroborates and extends previous studies. These data are also presented here.

II. EXPERIMENTAL PROCEDURES AND RESULTS

A. General

The ^{14}C beam was provided by the Brookhaven National Laboratory (BNL) tandem Van de Graaff facility. The target[10] was a silver foil, 1.27×10^{-3} cm thick, sulfided on one side with 300 μg/cm^2 of enriched sulfur (81.1% ^{36}S, 18.8% ^{34}S). It was assumed that the sulfur is confined to that surface depth necessary to combine 300 μg/cm^2 of sulfur with silver in the stoichiometric proportion of the stable compound Ag_2S. This gives an Ag_2S target thickness of 2.12 mg/cm^2 and an energy loss for 34-MeV ^{14}C ions of $\sim$4.3 MeV. Because of the ^{34}S in the target, some measurements were also made with a similar Ag_2S target fabricated from ^{34}S alone.

Gamma-ray spectra were collected with four Ge detectors: (1) an intrinsic Ge low-energy photon spectrometer (LEPS), (2) a Compton suppression spectrometer (CSS)

TABLE I. Relative production cross sections in $^{36}S+^{14}C$ for $E(^{14}C)=32$ MeV.

Outgoing channel	Residual nucleus	Transition (keV)	Cross section (mb)[a] CASCADE	Observed
2n	^{48}Ti	984	31	47
3n	^{47}Ti	159	440	(440)
pn	^{48}Sc	131	8	7
p2n	^{47}Sc	1147	100	42
αn	^{45}Ca	174[b]+1554[c]	21	25
α2n	^{44}Ca	1157	62	52

[a]The prediction of CASCADE (Ref. 9) is in mb, the observed relative cross section is normalized to that of CASCADE for ^{47}Ti.

[b]The $\frac{5}{2}^- \rightarrow \frac{7}{2}^-$ 174$\rightarrow$0 transition.

[c]This previously unobserved transition we identify as the ground state decay of an $(\frac{11}{2}^-)$ state at 1554.36(8) keV (see Sec. III C).

consisting of an intrinsic coaxial Ge detector and a NaI anticoincidence shield, (3) a second Compton suppression spectrometer (designated BGO) utilizing an intrinsic coaxial Ge detector and a bismuth germanate anticoincidence shield, and (4) a bare intrinsic coaxial Ge detector.

The γ-ray measurements included excitation functions, angular distributions, and $\gamma\gamma$ coincidences. The excitation function consisted of γ spectra at $E(^{14}C)=18$, 22, 26, 30, 34, and 38 MeV. At each energy LEPS and coaxial Ge spectra were recorded with detectors located at 90° to the beam and $\sim$10 cm from the target. The angular distributions were taken with the LEPS and CSS simultaneously at angles to the beam for each of 0°, 15°, 30°, 60°, 75°, and 90°. The $\gamma\gamma$ coincidences were recorded with the CSS at 90°, the BGO at 130°, and the bare Ge detector at 40°. Twofold coincidences were event-mode-recorded (EMR) onto tape and subsequentially analyzed for all three pairs of detectors. Both the angular distribution and $\gamma\gamma$-coincidence data provided useful Doppler shift attenuation (DSA) data which was analyzed to provide lifetime information. All procedures are similar to those used at BNL previously and explained in detail elsewhere.[11]

The excitation functions indicated that at $E(^{14}C)=34$ MeV useful information could be obtained on several channels (see Table I). All subsequent measurements were made at this energy.

B. ^{47}Ti

The experimental results for ^{47}Ti are summarized in Table II and Fig. 1. Figures 2 and 3 illustrate the $\gamma\gamma$-coincidence data upon which the decay scheme was based. The Doppler-shift lifetime information provided by these data is also apparent in these figures. Figure 4 illustrates the type of Doppler shift lifetime information which was obtainable from the angular distribution data.

The Doppler shift attenuation factor, $F(\tau)$, was extracted from the data and analyzed to determine the meanlife, τ, by procedures described in Ref. 11. In particular, allowance was made for feeding via higher levels. The alignment coefficients α_2 and α_4 necessary[11] for extracting the γ-ray multipole mixing ratio, $x(L+1/L)$, were evaluated from the 1285- and 1305-keV transitions assuming them both to be pure $E2$. Then, for each transition, proper account was taken of the attenuation due to the observed cascades into the initial state. In doing so, all were assumed to be pure multipoles of the lowest allowed multipolarity (i.e., the dominant multipole of Table II).

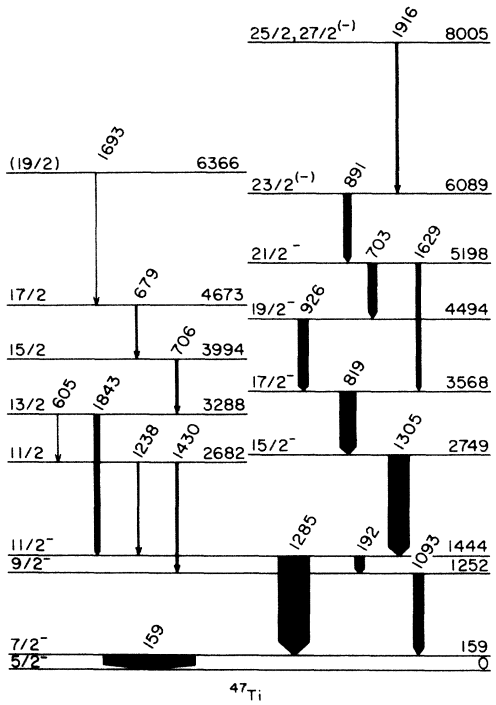

FIG. 1. Level scheme for ^{47}Ti showing excitation energies and γ-transition energies (in keV) for levels populated in the $^{36}S(^{14}C,3n\gamma)^{47}$Ti reaction only. The γ intensities are roughly proportional to the width of the arrows. Above the 1252-keV level there appear to be two groupings of levels; odd parity to the right and unknown (but tentatively assumed to be even) parity to the left. All transitions and levels are definitely placed except the somewhat uncertain 1693-keV transition and thus the 6366-keV level.

TABLE II. ^{47}Ti energy levels, γ-ray transitions, lifetimes, and multipole mixing ratios deduced from ^{36}S(^{14}C, 3n)^{47}Ti.

J_i^{π} [a]	E_i [b] (keV)	E_f (keV)	E_γ [c] (keV)	Angular distribution [d] I_γ	A_2 (%)	A_4 (%)	I_f [e] ($\times 10^{-2}$)	$F(\tau)$ [f] (%)	τ [g] Present (ps)	τ [g] Previous (ps)	Dominant [h] multipole	$x(L+1/L)$ [i] Present	$x(L+1/L)$ [i] Previous
$\frac{7}{2}^-$	159.369(20)	0	159.369(20)	92 320[2] [j]	−24(1)	0	499	0		301(8)	$M1$	+0.04(5)	+0.09(9) [l]
$\frac{9}{2}^-$	1252.098(35)	159	1092.710(50)	10 200[8]	−50(2)	0	35	71(4) [m]	0.17(4)	0.21(2)	$M1$	+0.36(15)	+0.29(3) [l]
		0	(1252.080) [k]	<3000									
$\frac{11}{2}^-$	1444.248(35)	1252	192.150(10)	4148[2]	−24(1)	0	109	7.4(4)	1.3(2)	1.5(5/3)	$M1$	+0.09(7)	−0.05(4) [n]
		159	1284.864(40)	32 200[2]	+31(2)	−7(2)					$E2$	[0]	
$\frac{11}{2}$	2682.336(53)	1444	(1238.070) [o]	1800[50] [o]			26		>10	6(>6/2.5)			
		1252	1430.215(40)	2970[3]	−25(2)	0		<2			($M1$)	+0.02(4)	+0.00(2)
$\frac{15}{2}^-$	2748.873(53)	1444	1304.606(40)	19 200[4]	+31(2)	−7(2)	25	10(1)	1.6(3)	3.2(28/1.2)	$E2$	[0]	
$\frac{13}{2}$	3287.723(82)	2682	605.470(50)	2220[20]	−51(15)	0	30		1.4(3)		($M1$)	+0.40(50)	+0.00(4)
		1444	1843.358(60)	4000[15]	−23(2)	0		14(1)			($M1$)	+0.00(6)	
$\frac{17}{2}^-$	3567.971(73)	2749	819.090(50)	16 700[5]	−40(2)	0	41	54(2)	0.10(3)	<0.39(11)	$M1$	+0.16(9)	+0.015(75) [n]
$\frac{15}{2}$	3993.934(96)	3288	706.211(50)	3200[20]	−65(15)	0	8	56(10)	0.14(11/7)		($M1$)	+3.0(30)	
$\frac{19}{2}^-$	4494.100(94)	3568	926.119(60)	9610[5]	−26(2)	0	52	59(2)	0.16(4)	<0.36(11)	$M1$	+0.05(4)	+0.05(4)
$\frac{17}{2}$	4672.90(12)	3993	678.948(80)	2430[15]	−50(15)	0	24	70(10)	0.18(8)		($M1$)	+0.40(50)	
$\frac{21}{2}^{(-)}$	5197.82(11)	4494	703.322(50)	9400[20]	−40(10)	0	47		0.07(5)		$M1$	+0.18(20)	
		3568	1629.83(40)	3000[20]				70(5)			$E2$	[0]	
$\frac{23}{2}^{(-)}$	6088.96(23)	5198	891.13(20)	5730[15]	−33(3)	0	43	75(5)	0.05(3)		$M1$	+0.09(8)	
$(\frac{19}{2})$	6366.1(15)	4673	1693.2(9)	400[30]			4	>80	<0.04		($M1$)		
$\frac{25}{2}, \frac{27}{2}^{(-)}$	8005.45(30)	6088	1916.45(20)	1400[15]	+20(10)	0	14	33(3)	0.70(15)		($M1$)	−0.30(40)	
											($E2$)	+0.00(30)	

TABLE II. (*Continued*).

[a]See the text for spin parity assignments.
[b]Corrected for recoil. The uncertainty in the least significant figure is given in parentheses.
[c]Not corrected for recoil. Energies enclosed in parentheses are calculated from $E_i - E_f$.
[d]The relative intensity I_γ is corrected for the relative γ-ray efficiency and is in arbitrary units. The numbers in square brackets under I_γ are the uncertainties in %. Results were extracted for unresolved multiplets using auxiliary information (excitation functions, coincidence data, etc.). An entry of 0 for A_4 means the fit was to $I_\gamma(1+A_2P_2(\theta_\gamma))$ only, i.e., χ^2 was not significantly improved by the inclusion of an A_4 term.
[e]Relative side feeding of the level in question in units of $100I_\gamma$.
[f]The Doppler shift attenuation factor (see the text).
[g]Mean life. Present results are derived from the $F(\tau)$ values as explained in the text. The previous results are from Ref. 5. In the case of asymmetric errors, the upper limit is given first.
[h]Entries in parentheses are assumed.
[i]The phase convention is that of Rose and Brink (Ref. 12). The J values of the first column are assumed. Values in square brackets are assumed.
[j]There is a small (unknown) contribution from $T_{1/2}=3.42d$ ^{47}Sc$(\beta^-)^{47}$Ti.
[k]Obscured by the 159- + 1093-keV sum peak.
[l]From Ref. 5.
[m]For the side feeding component only.
[n]Average of the values quoted in Refs. 6 and 8.
[o]Unresolved in singles from ^{45}Sc $127\rightarrow 0$. The intensity is estimated from the $\gamma\gamma$-coincidence data.

We first discuss the spin-parity assignments of Table II and Fig. 1. The lifetime results simplify discussion of the assignments. We assume that the recommended upper limits (RUL's) of Endt[13] for $A=6$–44 also pertain to $A=47$. These are 100 W.u. (Weisskopf units) for $E2$ and 3 W.u. for $M2$ transitions. Invoking the partial meanlifes inferred from Table II, we find that all transitions with $E_\gamma < 1000$ keV are dipole as are the 1093- and very probably the 1693-keV transitions. The 1693-, 1843-, and 1916-keV transitions are dipole or $E2$. If now we invoke the high selectivity for yrast states of the fusion-evaporation mechanism and the restrictions[11] on A_2 and A_4 for given J_i, J_f, and τ, we are led to the spin assignments of Table II and Fig. 1. We note that our experimental results as summarized in Table II are in excellent accord with those of previous workers.

The spin-parity assignments for the levels below 5-MeV excitation and to the right in Fig. 1 were made previously[5] and we adopt them without additional discussion except to note that our results are in complete agreement and support these assignments. The levels above 5-MeV excitation are newly assigned in this study. The angular distributions of the 703- and 891-keV transitions fix them as $J\pm1\rightarrow J$ and we invoke the reaction mechanism to decide on $J+1\rightarrow J$. From the RUL, the 1629-keV transition is too fast to be $M2$ and so the 5198-keV level is assigned $J^\pi=\frac{21}{2}^-$. The probable odd-parity assignment for the 6089-keV level is based on predictions[1,2] of the $(f_{7/2})^n$ shell model and thus is model dependent. The positive anisotropy and the rather long meanlife of the 1916-keV transition lead us to suggest $E2$ character and $\frac{27}{2}^-$ for the 8005-keV level.

The levels above 3.3-MeV excitation and to the left in Fig. 1 result from this study. Systematics of neighboring nuclei favor even parity for the levels above 2.5 MeV in this group. In addition, Meyer-Schützmeister *et al.*[7] demonstrated very poor agreement with shell-model predictions if the 2682-keV level has odd parity. These suggested even-parity assignments are at variance with the odd parity suggested by Sawa *et al.*[6] for the 2682- and 3288-keV levels. We stress that there is no experimental evidence from either Ref. 6 or the present results to favor either parity for these two levels. Sawa *et al.*[6] observed a 1228-keV $J\pm1\rightarrow J$ transition from a 2672-keV level to the $\frac{11}{2}^-$ 1444-keV transition and gave the 2672-keV level a probable $\frac{13}{2}^-$ assignment. We can see no reason to prefer odd parity over even. In addition, the nonappearance of this transition in the present study strongly suggests $J=\frac{9}{2}$ rather than $\frac{13}{2}$.

C. ^{47}Sc

The only previous significant study of the yrast spectrum of ^{47}Sc is that of Toulemonde *et al.*[14] who observed levels up to 2644-keV excitation via the ^{44}Ca$(\alpha,p\gamma)^{47}$Sc reaction. As summarized in Fig. 5 and Table III the ^{36}S$(^{14}$C,2n$p\gamma)^{47}$Sc reaction is highly selective but two additional levels were observed at 3303 and 3867 keV. An example of the $\gamma\gamma$-coincidence data for this nucleus is shown in Fig. 6. Analysis of the data summarized in Table III was complicated because of complexities in the

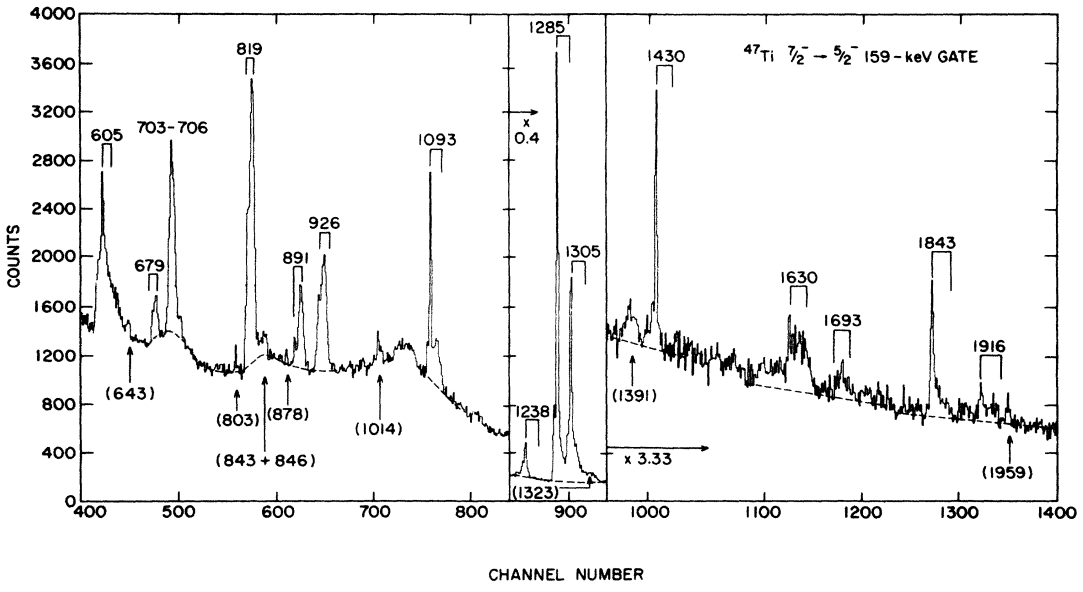

FIG. 2. Portions of a 2048-channel spectrum in coincidence with the 159-keV $\frac{7}{2}^- \rightarrow \frac{5}{2}^-$ ground-state transition in ^{47}Ti. The displayed spectrum is that of the bare Ge detector at 40° to the beam. The spectrum was gated by the CSS detector (90° to beam). ^{47}Ti γ transitions are identified by their energies in keV. The transitions with energies in parentheses labeled below the data are either unidentified or known contaminants [e.g., the 843- and 1014-keV lines are in ^{27}Al and are presumed to arise from (n,n') events associated with the 3nγ channel]. The γ transitions of 605 and 703—706 keV are on backgrounds due to the well-known Ge neutron edges at 596 and 691 keV, respectively. The only identified ^{47}Ti transition not shown is that of 192 keV. Most of the ^{47}Ti lines have obvious Doppler shapes. The expected extent of the Doppler line shapes is indicated by the double vertical lines above the peaks: these data were used to obtain some of the $F(\tau)$ values of Table II.

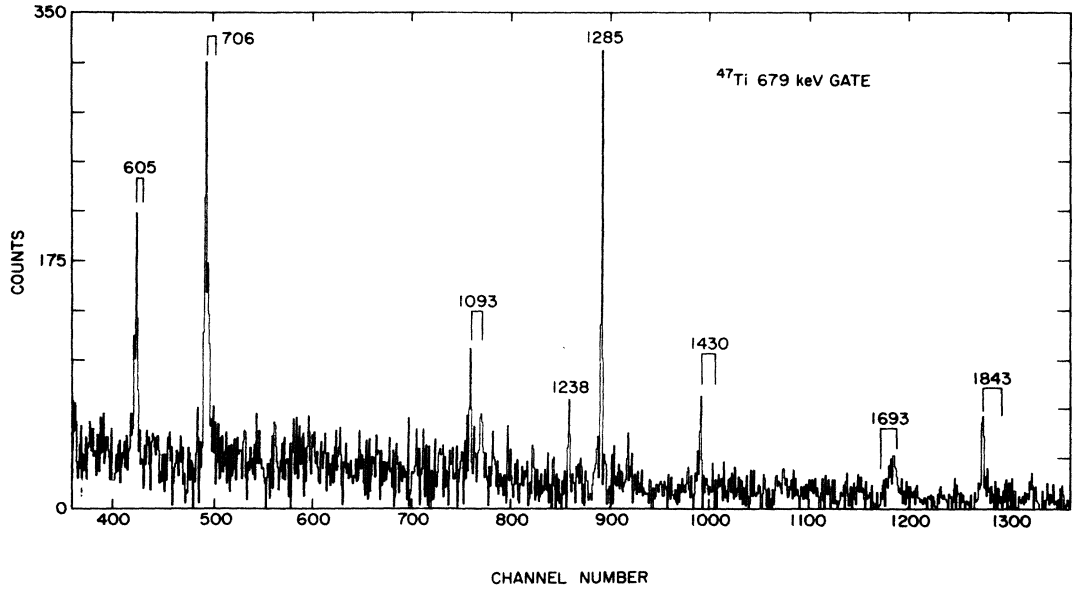

FIG. 3. A $\gamma\gamma$-coincidence spectrum similar to that illustrated in Fig. 2 but gated by the 679-keV transition in ^{47}Ti.

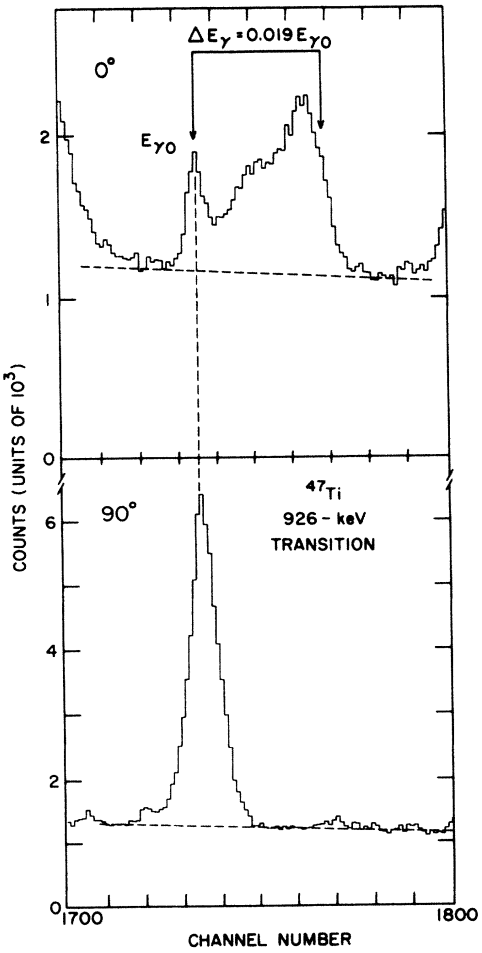

FIG. 4. Portions of 90° and 0° angular distribution spectra displaying the Doppler line shape of the ^{47}Ti 926-keV transition.

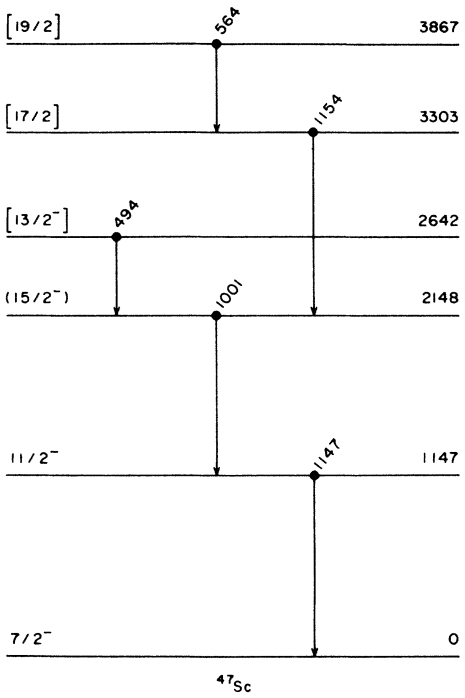

FIG. 5. Level scheme for ^{47}Sc showing excitation energies and γ-transition energies (in keV) for levels populated in the ^{36}S(^{14}C,2npγ)^{47}Sc reaction only. The spin-parity assignment for the 1147-keV level is from Ref. 5. The other assignments are discussed in the text.

spectra. For instance, the ^{47}Sc 2148→1147 transition was degenerate with the ^{44}Ca 3285→2283 transition (see Fig. 7) and the Doppler shifting ^{47}Sc 3303→2148 transition moved across the 1147-keV transition and the ^{44}Ca 1157-keV transition (see Fig. 7) as a function of θ_γ. An upper limit of 10% can be placed on the crossover 3867→2148 transition. As summarized in Table III, $F(\tau)$ values were obtained as well as some useful angular distribution data, in spite of the complexities encountered.

D. ^{44}Ca

The ^{44}Ca yrast scheme constructed from the present results on the ^{36}S(^{14}C,2n$\alpha\gamma$)^{44}Ca reaction is shown in Fig. 7. The data upon which this scheme is based are summarized in Table IV. All the transitions shown were observed previously. The levels up to the 6^+ level at 3285 keV have been formed in many reactions.[15] The decay of the $J^\pi=5^-$ 3913-keV state was first observed in the ^{43}Ca(n,γ)^{44}Ca reaction.[19] All the ^{44}Ca transitions observed in the present study were also observed in the ^{28}Si(^{19}F,3pγ)^{44}Ca reaction although the decays from the (8^+) and 5^- states were unidentified in the report[17,18] of that work. The 5088→3285 transition was also observed in the ^{30}Si(^{16}O,2pγ)^{44}Ca reaction[20] but no angular distribution or lifetime results were reported from that study. Upper limits of 10% can be placed on decays of the 3285-

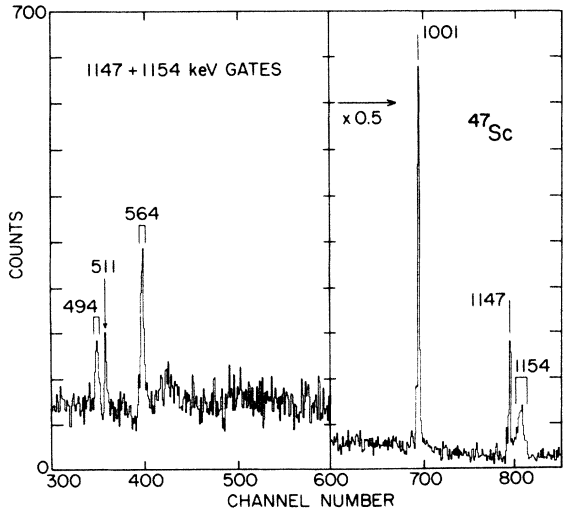

FIG. 6. A $\gamma\gamma$-coincidence spectrum gated by the 1147- and 1154-keV ^{47}Sc transitions (see Fig. 5).

TABLE III. ^{47}Sc energy levels, γ-ray transitions, lifetimes, and multipole mixing ratios from ^{36}S(^{14}C,2np)^{47}Sc.

				Angular distribuion[d]					τ[g]				
J_i^{π}[a]	E_i[b] (keV)	E_f (keV)	E_γ[c] (keV)	I_γ	A_2 (%)	A_4 (%)	I_f[e] ($\times 10^{-2}$)	$F(\tau)$[f] (%)	Present (ps)	Previous (ps)	Dominant[h] multipole	$x(L+1/L)$[i] Present	$x(L+1/L)$[i] Previous[j]
$\frac{11}{2}^-$	1146.989(40)	0	1146.974(40)	8824[2]	+29(2)	−8(2)	18	<5	>1.2	4.5(16)	$E2$	0.00(6)	−0.02(3)
$(\frac{15}{2}^-)$	2148.2(5)	1147	1001.2(5)[k]	7000[10][l]	>0[m]	0	16	<5	>6	>3	$E2$		−0.10(13)
$[\frac{13}{2}^-]$	2641.9(5)	2148	493.66(10)	1240[5]	−18(2)	0	12	44(4)	0.46(9)	0.58(42)	($M1$)	0.00(6)	−0.04(8)
		1879	(763.0)	<400									
		1147	(1494.9)	<1450									
$[\frac{17}{2}]$	3302.5(10)	2148	1154.3(9)	4120[6]	<0[n]	0	16	58(4)	0.10(4)		($M1$)		
$[\frac{19}{2}]$	3867.0(11)	3303	564.46(30)	2540[7]	<0[n]	0	25	55(4)	0.30(8)		($M1$)		

[a]See the text. Parentheses denote probable assignments. Square brackets denote speculations.
[b]Corrected for recoil. The uncertainty in the least significant figure is given in parentheses.
[c]Not corrected for recoil. Energies enclosed in parentheses are calculated from $E_i - E_f$.
[d]The relative intensity I_γ is corrected for the relative γ-ray efficiency and is in arbitrary units. The numbers in square brackets under I_γ are the uncertainties in (%). Results were extracted for unresolved multiplets using auxiliary information (excitation functions, coincidence data, etc.). An entry of 0 for A_4 means the fit was to $I_\gamma(1+A_2P_2(\theta_\gamma))$ only, i.e., χ^2 was not significantly improved by the inclusion of an A_4 term.
[e]Relative side feeding of the level in question in units of $100I_\gamma$.
[f]The Doppler shift attenuation factor (see the text).
[g]Mean life. Present results are derived from the $F(\tau)$ values as explained in the text. The previous reuslts are from Ref. 5.
[h]Entries in parentheses are assumed.
[i]The phase convention is that of Rose and Brink (Ref. 12). The J values of the first column are assumed.
[j]Reference 14.
[k]From the $\gamma\gamma$-coincidence data.
[l]Obscured in singles by the ^{44}Ca $6_1^+ \rightarrow 4_1^+$ transition (see Table IV).
[m]Assuming the ^{44}Ca 1002-keV transition is pure $E2$ (see Table IV).
[n]The spectra are complex and the transitions Doppler shifted, hence only these limits were obtained.

TABLE IV. ^{44}Ca energy levels, γ-ray transitions, lifetimes, and multipole mixing ratios from ^{36}S(^{14}C,2nα)^{44}Ca.

				Angular distribution[d]					τ[g]				
J_i^{π}[a]	E_i[b] (keV)	E_f (keV)	E_γ[c] (keV)	I_γ	A_2 (%)	A_4 (%)	I_f[e] ($\times 10^{-2}$)	$F(\tau)$[f] (%)	Present (ps)	Previous (ps)	Dominant[h] multipole	$x(L+1/L)$[i] Present	Previous
2^+	1157.047(15)	0	1157.031(15)[j]	9687[3]	+31(1)	−5(1)	25			4.2(3)	$E2$		
4^+	2283.155(43)	1157	1126.092(40)[j]	6780[2]	+31(1)	−7(1)	11			2.8(10)	$E2$	+0.00(4)	+0.054(4)
4^+	3044.35(20)	2283	761.19(20)	485[5]	+25(3)	+10(5)	~0			6.7(16)	$M1$	+0.18(8)	+0.25(20)
		1157	1887.45(20)	415[5]	+32(7)	−23(7)					$E2$	+0.04(22)	+0.08(5)
6^+	3285.018(53)	2283	1001.850(31)[j]	5700[20][k]	+35(1)	−6(1)	17			19.4(15)	$E2$	+0.00(8)[l]	
5^-	3913.55(10)	3285	628.53(9)	1300[10]	+22(3)	−4(5)	26	<10	>3		$E1$	+0.30(14)	
		3044	(869.19)[m]	≤900[7][n]							$E1$		
$(8)^+$	5087.648(96)	3285	1802.59(8)	2900[10]	+34(4)	−5(5)	29	31(7)	0.77(20)		($E2$)	−0.01(6)	

[a]See text.
[b]Corrected for recoil. The uncertainty in the least significant figure is given in parentheses.
[c]Not corrected for recoil. Energies enclosed in parentheses are calculated from $E_i - E_f$.
[d]The relative intensity I_γ is corrected for the relative γ-ray efficiency and is in arbitrary units. The numbers in square brackets under I_γ are the uncertainties in (%). Results were extracted for unresolved multiplets using auxiliary information (excitation functions, coincidence data, etc.). An entry of 0 for A_4 means the fit was to $I_\gamma(1+A_2P_2(\theta_\gamma))$ only, i.e., χ^2 was not significantly improved by the inclusion of an A_4 term.
[e]Relative side feeding of the level in question in units of $100I_\gamma$.
[f]The Doppler shift attenuation factor (see the text).
[g]Mean life. Present results are derived from the $F(\tau)$ values as explained in the text. Previous results are from Ref. 15.
[h]Entries in parentheses are assumed.
[i]The phase convention is that of Rose and Brink (Ref. 12). The J values of the first column are assumed. The previous values are from Ref. 15.
[j]From Ref. 16.
[k]Unresolved from the more intense ^{47}Sc 2148→1147 transition (see the text).
[l]From analysis of the data of Refs. 17 and 18 (see the text).
[m]Unresolved from the more intense ^{45}Sc 2107→1237 transition.
[n]The intensity limit is from the decay of the 4_2^+ level. The limit was assumed in calculating the branching ratios shown in Fig. 7 for the 3914-keV level.

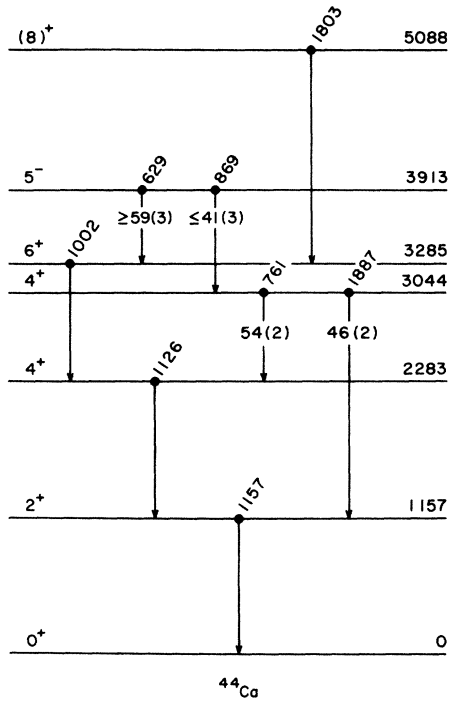

FIG. 7. Level scheme for ^{44}Ca showing excitation energies and γ-transition energies (in keV) for levels populated in the ^{36}S(^{14}C,2n$\alpha\gamma$)^{44}Ca reaction.

and 3913-keV levels to the 3044-keV level.

The spin-parity assignments for all levels save the 3285- and 5088-keV levels are from Endt and van der Leun.[15] For the 3285-keV level, $J^\pi=5^+$ or 6^+ were allowed by that evaluation. The present data for the 3285→2283 transition is not very useful because there are two nearly equal contributions to the 1002-keV γ-ray peak, the other being from ^{47}Sc (Table III). However, the data from ^{28}Si+^{19}F taken previously[17,18] at the BNL tandem facility includes γ-ray linear polarization data and when those angular distribution and linear polarization data are analyzed simultaneously by conventional methods,[11] the $J^\pi=5^+$ alternative for the 3285-keV level is rejected at the 0.1% probability level while the 6^+ alternative gives a good solution for $x(M3/E2)=+0.00(8)$ as shown in Table IV.

The spin parity of the 5088-keV level cannot be rigorously determined from the present study. Acceptable solutions to the angular distribution of the 1803-keV level are found for $J=4$, 5, 6, and 8. $J=7$ can be rejected at the 95% confidence level. However, the reaction mechanism strongly favors $J>6$ for this level since it is quite strongly formed in this and the previous heavy-ion studies. Thus we have a strong preference for $J=8$. The $J=5$–7 solutions are for sizable values of the quadrupole/dipole mixing ratio such that for any J the RUL (Ref. 13) for $M2$ transitions (3 W.u.) is exceeded for odd parity. Thus, a definite even-parity assignment can be made.

The decay of the 5^- 3913-keV level is quite surprising. There is no evidence of a Doppler shift, hence the lifetime limit of Table IV. The positive A_2 value for the 629-keV transition demands a sizable $M2$ component. This suggests a highly retarded $E1$ transition and a lifetime in the ~1–10 ns range. We shall return to this interesting point later.

E. ^{45}Ca

The decay scheme constructed for ^{45}Ca from the present study of ^{36}S(^{14}C,n$\alpha\gamma$)^{45}Ca is shown in Fig. 8 and summarized in Table V. No yrast decays had been previously observed for this nucleus. The γ transitions shown were identified with ^{45}Ca on the basis of the excitation function, nonappearance in ^{34}S+^{14}C, and from the agreement in excitation energy with the high-spin $(f_{7/2})^5$ states proposed at 1562(8) and 2877(8) keV by Nann, Mueller, and Kashy.[21] These authors studied the ^{48}Ca(^{3}He,^{6}He) reaction and identified high-spin $(f_{7/2})^5$ states from angular distributions and relative cross sections. There is no ambiguity in the identification of the cascade of 1324-1554 keV corresponding to these two levels. Using the alignment parameters determined for ^{47}Ti and ^{47}Sc, the angular distributions of the two transitions are found to be in good agreement with a stretched $\frac{15}{2}^- \rightarrow \frac{11}{2}^- \rightarrow \frac{7}{2}^-$ cascade. For the 1554→0 transition $\frac{9}{2} \rightarrow \frac{7}{2}$ is excluded at the 0.1% probability level. Other $J \rightarrow \frac{7}{2}^-$ transitions

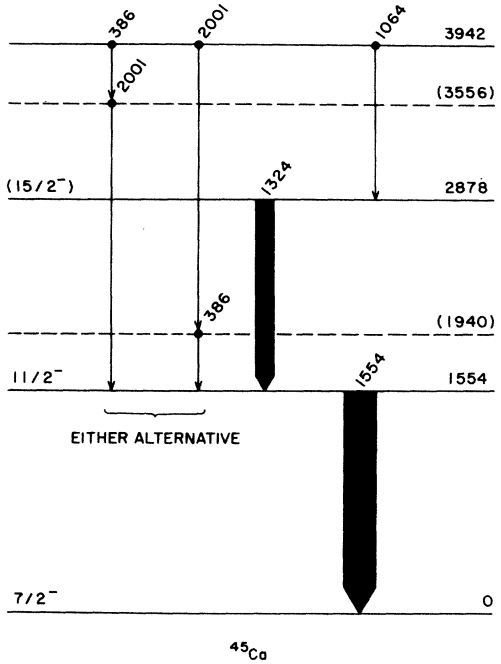

FIG. 8. Level scheme for ^{45}Ca showing excitation energies and γ-transition energies (in keV) for levels populated in the ^{36}S(^{14}C,n$\alpha\gamma$)^{44}Ca reaction. The γ intensities are roughly proportional to the widths of the arrows. The 386- and 2001-keV transitions have equal intensities within the uncertainties and no discernable Doppler shifts. Thus, two possible placings of the intermediate level are shown for the cascade of these two transitions.

TABLE V. ^{45}Ca energy levels, γ-ray transitions, lifetimes, and multipole mixing ratios deduced from ^{36}S(^{14}C,nα)^{45}Ca.

					Angular distribution[d]						
J_i^{π}[a]	E_i[b] (keV)	E_f (keV)	E_γ[c] (keV)	I_γ	A_2 (%)	A_4 (%)	I_f[e] ($\times 10^{-2}$)	$F(\tau)$[f] (%)	τ[g] (ps)	Dominant[h] multipole	$x(L+1/L)$[i]
$(\frac{11}{2}^-)$	1554.366(80)	0	1554.337(80)	3570[2]	+29(2)	−7(3)	17	<5	>3	*E*2	+0.00(6)
$(\frac{15}{2}^-)$	2877.99(12)	1554	1323.60(9)	1590[4]	+28(2)	−9(3)	13	<8	>3	*E*2	+0.00(6)
	3555.89(13)	1554	2001.48(10)	250[30]	−8(17)	0	0				
	3941.70(12)	3556	385.74(8)[j]	250[50][j]	−38(4)	−2(7)	6	<10	>3		
		2878	1063.83(6)[k]	300[50][k]	+68(9)	−11(12)		<10			

[a]See the text.

[b]Corrected for recoil. The uncertainty in the least significant figure is given in parentheses.

[c]Not corrected for recoil.

[d]The relative intensity I_γ is corrected for the relative γ-ray efficiency and is in arbitrary units. The numbers in square brackets under I_γ are the uncertainties in (%). Results were extracted for unresolved multiplets using auxiliary information (excitation functions, coincidence data, etc.). An entry of 0 for A_4 means the fit was to $I_\gamma(1+A_2P_2(\theta_\gamma))$ only, i.e., χ^2 was not significantly improved by the inclusion of an A_4 term.

[e]Relative side feeding of the level in question in units of $100I_\gamma$.

[f]The Doppler shift attenuation factor (see the text).

[g]Mean life. Present results are derived from the $F(\tau)$ values as explained in the text.

[h]Assumed.

[i]The phase convention is that of Rose and Brink (Ref. 12). The J values of the first column are assumed.

[j]E_γ is from the LEPS spectra in which this and a 386.44-keV γ ray of comparable intensity were resolved. The angular distribution is for the unresolved doublet observed in the Ge spectra. $F(\tau)$ and τ are for this ^{45}Ca transition.

[k]There is some evidence that this γ ray contains an unresolved contaminant, also of $I_\gamma \sim 300$. E_γ, A_2, A_4 are for the composite peak, I_γ is estimated from the $\gamma\gamma$ spectra.

with $J=\frac{7}{2}$ to $\frac{3}{2}^-$ are possible but disfavored. A similar statement can be made for the 1324-keV transition with $J=\frac{13}{2}$ excluded at the 0.1% limit and $J=\frac{11}{2}-\frac{7}{2}$ disfavored, all assuming $\frac{11}{2}^-$ for the 1554-keV level. Neither transition showed any Doppler effects, hence the limits on τ.

The other three transitions shown were relatively weak and two of them were plagued by experimental problems (see Table V). Thus, the spin parity and placement of the two levels is not determined, as indicated in Fig. 8.

F. ^{48}Ti

The decay scheme constructed from the present results for ^{48}Ti is shown in Fig. 9. The decay scheme follows (independently) the very comprehensive ^{45}Sc(α,pγ)^{48}Ti results of Glatz *et al.*[4] whose spin-parity assignments and branching ratios are shown.

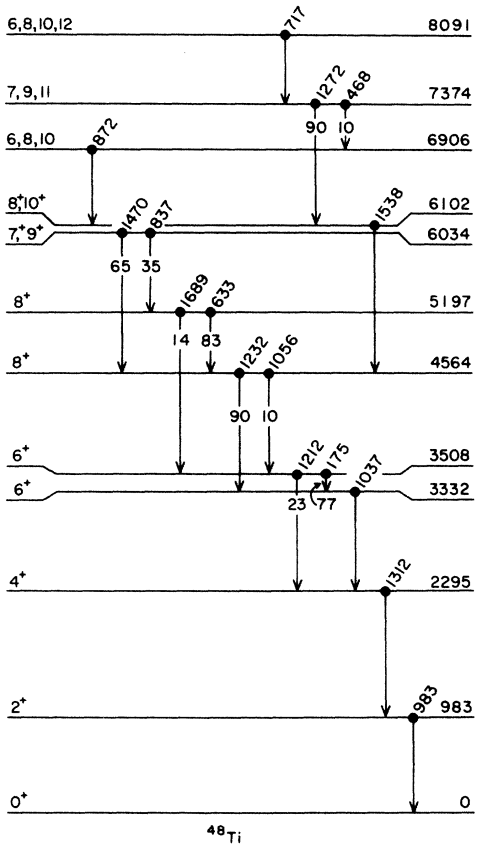

FIG. 9. Level scheme for ^{48}Ti showing excitation energies and γ-transition energies (in keV) for levels populated in the ^{36}S(^{14}C,2nγ)^{48}Ti reaction. The spin-parity assignments are from the ^{45}Sc(α,pγ)^{48}Ti results of Glatz *et al.* (Ref. 4). They are from angular correlation and lifetime results only. Glatz *et al.* give model dependent arguments to support the higher spin alternative and even parity for all levels shown. Only transitions observed in the present work are shown. The branching ratios (in %) are those of Ref. 4, to which the reader is referred for more detailed results.

High-spin states of ^{48}Ti were also examined by Fortuna *et al.*[22] using the ^{48}Ca(^{3}He,3nγ)^{48}Ti and ^{44}Ca(^{7}Li,2npγ)^{48}Ti reactions. They observed the same levels up to the 8^+ 4564-keV level but then proposed a

$$6735 \xrightarrow{633} 6102 \xrightarrow{1538} 4564$$

cascade. We agree with Glatz *et al.*[4] that the 633-keV transition should be placed instead as 5197→4564, i.e., there is no 6735-keV level.

Glatz *et al.*[4] followed the argument of Fortuna *et al.*[22] that the selective nature of the heavy ion fusion evaporation reaction, i.e., ^{44}Ca+^{7}Li, favors yrast states and thus, in this case, the 10^+ assignment for the 6102-keV level. On the basis of this argument, Glatz *et al.*[4] could also eliminate the lower spin alternative for the levels above 6200 keV in Fig. 9 since they are predicated on 8^+ for the 6102-keV level. Our results strongly support this argument since the ^{35}S + ^{14}C reaction is even more selective of high spin than ^{44}Ca+^{7}Li. To illustrate this selectivity, note that Glatz *et al.*[4] placed 214 ^{48}Ti levels below 8100 keV via the (α,pγ) reaction while we observed only the 11 shown in Fig. 9. Thus, in the discussion to follow, we confidently assume the highest spin alternatives for the

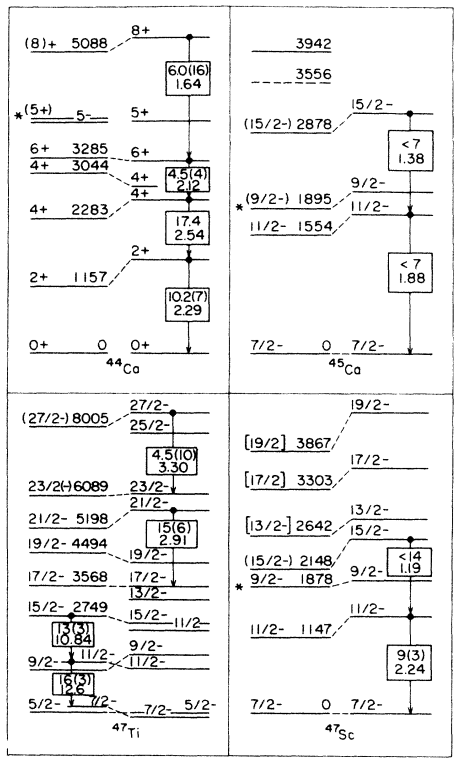

FIG. 10. Comparison of the experimental yrast spectra with the $(f_{7/2})^n$ predictions of Ref. 2. Levels marked by an asterisk were not observed in the present study. The numbers in rectangular boxes are experimental (top) and predicted (bottom) $E2$ transition strengths in W.u.

levels above 6 MeV in Fig. 9.

Glatz *et al.*[4] reported Doppler shift lifetime results for all levels of Fig. 9 except for the highest two, i.e., the 7374- and 8091-keV levels. For the decay of both of these we observed partial Doppler shifts: $F(\tau)=0.57(10)$ and 0.73(10) for the 717- and 1272-keV transitions, respectively. From these we deduce lifetime estimates of 0.3(1) and 0.04(6) ps for the 8091- and 7374-keV levels, respectively. The latter can be interpreted as a limit $\tau<0.16$ ps at the 90% confidence limit.

III. COMPARISON TO SHELL MODEL PREDICTIONS

A. The pure $(f_{7/2})^n$ model

1. The yrast spectra

We start our comparison to shell-model predictions with a comparison to the predictions of the empirical $(f_{7/2})^n$ model of Kutschera, Brown, and Ogawa.[2] Energy spectra for four of the nuclei studied are shown in Fig. 10. (A comparison for ^{48}Ti was made in Ref. 4.) The model energies for the yrast spectra are matched with our experimental determinations, probabilities, or speculations for the lowest-lying normal-parity level of each spin. The agreement is quite impressive.

2. E2 transitions

Also shown in Fig. 10 in the rectangular boxes are the experimental (top) and predicted (bottom) $E2$ transition strengths in Weisskopf units of most of the known $E2$ transitions. Here the agreement is not so impressive. The model uses effective charges of $\delta_n=\delta_p=0.9$ where the proton and neutron charges are $(1+\delta_p)e$ and $\delta_n e$, respectively. These were determined by comparison to known $6^+\rightarrow4^+$ and $\frac{15}{2}^-\rightarrow\frac{11}{2}^-$ transitions in $(f_{7/2})^n$ nuclei. Thus the general trend, seen in Fig. 10, for the predictions to underestimate the $E2$ strengths seems quite surprising. We expect the $(f_{7/2})^n$ model calculations to be most accurate for the higher spin states. Thus, the disagreement is most surprising for the ^{48}Ca $8^+\rightarrow6^+$ and ^{47}Ti $\frac{21}{2}^-\rightarrow\frac{19}{2}^-$ transitions for which we have described the lifetime measurements.

3. M1 transitions

A comparison of our measurements of $M1$ transition strengths in ^{47}Ti, ^{47}Sc and ^{48}Ti is shown in Table VI; Kutschera *et al.*[2] used effective g factors selected to give

TABLE VI. Comparison of some measured $M1$ transition strengths with the $(f_{7/2})^n$ predictions of Ref. 2.

J_i^π[a]	E_i (keV)	J_f[a]	E_f (keV)	E_γ (keV)	$B(M1)_{\text{w.u.}}$[b] Expt.	Ref. 2
			^{47}Ti			
$\frac{7}{2}^-$	159	$\frac{5}{2}^-$	0	159	0.026(1)	0.0045
$\frac{9}{2}^-$	1252	$\frac{7}{2}^-$	159	1093	0.10(2)	0.0045
$\frac{11}{2}^-$	1444	$\frac{9}{2}^-$	1252	192	0.41(7)	0.168
$\frac{17}{2}^-$	3568	$\frac{15}{2}^-$	2749	819	0.6(2)	0.569
$\frac{19}{2}^-$	4494	$\frac{17}{2}^-$	3568	926	0.25(6)	0.743
$\frac{21}{2}^-$	5198	$\frac{19}{2}^-$	4494	703	0.34(12)	0
$\frac{23}{2}^{(-)}$	6089	$\frac{21}{2}^-$	5198	891	0.9(5)	0.883
$(\frac{25}{2}^-)$	8005	$\frac{23}{2}$	6089	1916	0.0064(14)	0.0045
			^{47}Sc			
$(\frac{13}{2}^-)$	2642	$(\frac{15}{2})^-$	2148	494	$\leq$0.57(11)[c]	2.078
$(\frac{13}{2}^-)$	2642	$\frac{11}{2}^-$	1147	1495	$<$0.02[d]	0.307
$(\frac{17}{2}^-)$	3303	$(\frac{15}{2}^-)$	2148	1154	0.21(8)	1.087
$(\frac{19}{2}^-)$	3867	$(\frac{17}{2}^-)$	3303	564	0.59(16)	0.990
			^{48}Ti			
(11^+)	7374	(10_1^+)	6102	1272	$>$0.2	0
(11^+)	7374	(10_2^+)	6906	468	$>$0.2	2.074
(12^+)	8091	(11^+)	7374	717	0.29(10)	1.344

[a] J^π values in parentheses are assumed for purposes of this comparison.

[b] The $B(M1)$ were extracted from experiment assuming negligible $E2$ contributions. This assumption is consistent with the observed and previously known $E2/M1$ mixing ratios.

[c] This value corresponds to a 100% branching ratio.

[d] The limit corresponds to $\leq$54% for the branching ratio (see Table III).

best agreement with experimental odd proton and odd neutron ground state g factors. Thus, once again, we expect rather good agreement. For the stronger transitions [$B(M1) > 0.2$ W.u.] the agreement for ^{47}Ti is reasonable. For ^{47}Sc and ^{48}Ti it is poor. (The predictions for weak transitions are not reliable because of the truncated configurational space.)

4. Discussion

^{44}Ca. As discussed in Sec. II D, the A_2 value of $+0.22(3)$ for the $5^- \rightarrow 6^+$ transition gives $x(M2/E1) = +0.30(14)$. If now we invoke the RUL of 3 W.u. for $M2$ transitions we are led to a limit of >0.18 ns for the meanlife of the 3914-keV level. This in turn implies a retardation for the $E1$ $5^- \rightarrow 6^+$ transitions of $>10^5$ and even more for the $5^- \rightarrow 4_1^+$ and $5^- \rightarrow 4_2^+$ transitions. The 5^- 3914-keV level presumably arises mainly from $d_{3/2}^{-1} f_{7/2}^5$ (see Sec. III B). Since $d_{3/2} \leftrightarrow f_{7/2}$ $E1$ transitions are forbidden, retardation of the $E1$ decays of the 3914-keV level to the two 4^+ levels and the 6^+ level below it, is expected. A lifetime measurement of the 3914-keV level would be valuable since it would determine this retardation. It should be kept in mind, however, that the possibility exists that the 3914-keV level is actually $J^\pi = 5^+$, the 3923-keV level is $J^\pi = 5^-$ (see Fig. 10), and the various pieces of experimental information[15] bearing on this close-lying doublet have somehow become confused. In this regard, we note that in the $(f_{7/2})^n$ model, $M1$ transitions between the 5_1^+ state and other $(f_{7/2})^n$ states are forbidden by the seniority selection rule.[2]

^{47}Sc. We have tentatively suggested $\frac{13}{2}^-$ for the 2642-keV level because of the $(f_{7/2})^n$ predictions (Fig. 10) for its energy. A difficulty with this assignment is the absence of a dominant decay to the $\frac{11}{2}^-$ state at 1147 keV (see Table VI). Because of this anomaly, the $\frac{13}{2}^-$ suggestion is quite speculative indeed.

^{47}Ti. There are two anomalies in the $M1$ $J+1 \rightarrow J$ cascade ending at the $\frac{15}{2}^-$ level. First, there is only one $E2$ crossover, and second, we have speculated that the $\frac{25}{2}^-$ level is not formed with sufficient intensity to be observed. As regards the first anomaly, the predicted[2] branching ratios for the $E2$ crossover transitions are $\frac{25}{2}^- \rightarrow \frac{21}{2}^-$ (6%), $\frac{23}{2}^- \rightarrow \frac{19}{2}^-$ (3%), $\frac{21}{2}^- \rightarrow \frac{17}{2}^-$ (100%), and $\frac{19}{2}^- \rightarrow \frac{15}{2}^-$ (5%). Since branches $<10\%$ would easily be overlooked, these predictions are consistent with observation.

As regards the second anomaly, we see from Fig. 10 that the lifetime of the 8005-keV level is in satisfactory agreement with that expected assuming the 8005-keV level were $\frac{27}{2}^-$ and decayed by a 100% branch to the 6089-keV level. Actually, the calculated branching ratio for an $E2$ $\frac{27}{2}^- \rightarrow \frac{23}{2}^-$ 8005$\rightarrow$6089 transition (with the $\frac{25}{2}^-$ level assumed at 7830 keV) is 81%. The small branch to the $\frac{25}{2}^-$ level would be below our detection threshold. So would the $\frac{25}{2}^- \rightarrow \frac{23}{2}^-$ transition if it had an intensity $\lesssim 0.5$ times that of the 8005$\rightarrow$6089 transition. We conclude that a comparison with $M1$ and $E2$ transition strengths gives good agreement with the suggested identification of $(f_{7/2})^7$ states of ^{47}Ti shown in Fig. 10.

B. Non-normal yrast states

The appearance of low-lying $\frac{3}{2}^+$ states in many odd-A $f_{7/2}$-shell nuclei signals the participation of the $(sd)^{-1}(fp)^{n+1}$ configuration. We are interested in the excitation energies of the yrast states of this configuration relative to the normal, i.e., $(fp)^n$, yrast states. For the calculation of non-normal high-spin yrast spectra the configurational space of $1d_{3/2}$-$1f_{7/2}$ should reproduce the main features even though it is surely severely truncated. We use an effective interaction developed by Wildenthal[23] for use in the upper part of the (s,d) shell. Calculations were performed using the computer program OXBASH (Ref. 24) in the model space $[(d_{3/2})^{-n}(f_{7/2})^{A+n-40};\ n=0,\ldots,m]$ with $m=3$ and 4 for non-normal and normal parity states, respectively. The resulting yrast spectra are compared to experiment in Figs. 11–15. In these figures the experimental data not discussed in this paper are taken from the appropriate compilation, i.e., $A=44$ (Ref. 15), $A=45$ (Ref. 25), $A=47$ (Ref. 5), and $A=48$ (Ref. 26). However, the spin parities in parentheses often represent only one choice of a range of possibilities. The shell-model predictions are labeled $D3F7$ and separated into normal (left-hand side) and non-normal (right-hand side) levels.

The calculations give a very consistent and reasonable explanation of the known non-normal parity states. The agreement with experiment for these states is as good as for the normal parity states; both predicted spectra are, in general, too expanded. To a lesser extent, this was also a feature of the pure $f_{7/2}$-shell calculation (Fig. 10). We now consider some specific features for each nucleus in turn.

^{44}Ca. The suggested 1^-, 4^-, and 2^- assignments to the experimental[15] levels at 3676, 3712, and 3776 keV, respec-

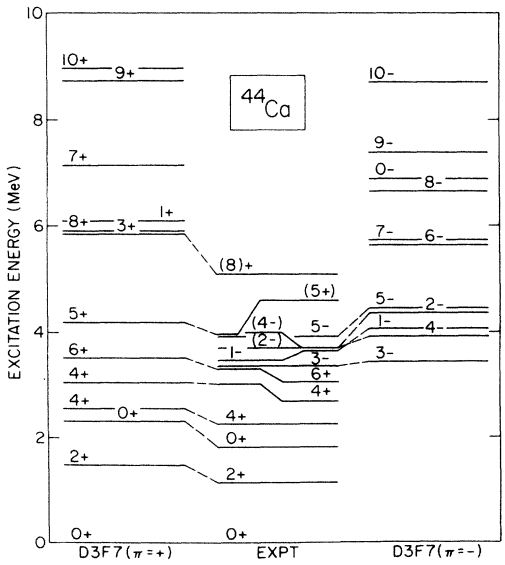

FIG. 11. Experimental and predicted (labeled $D3F7$) yrast spectra of ^{44}Ca. The model space is $[(d_{3/2})^{-n}(f_{7/2})^{A+n-40};\ n=0,\ldots,m]$ with $m=3$ or 4.

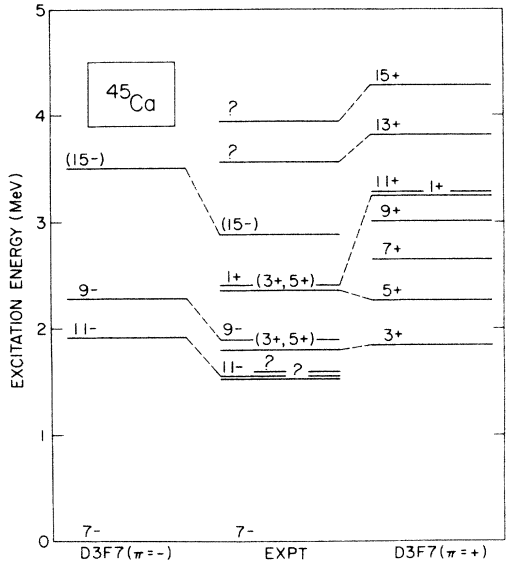

FIG. 12. Experimental and predicted yrast spectra of ^{45}Ca. See the caption of Fig. 11. Note that the levels are labeled by $2J$ and π.

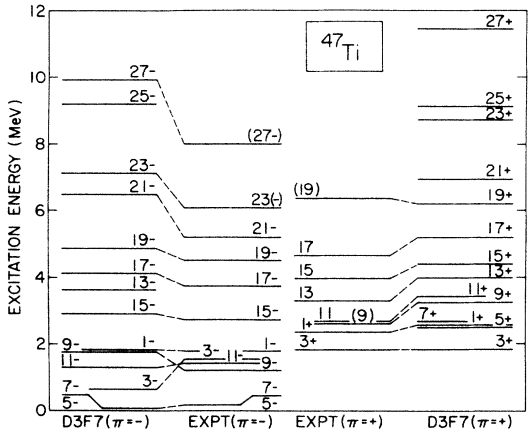

FIG. 14. Experimental and predicted yrast spectra of ^{47}Ti. See the caption of Fig. 11. Note that the levels are labeled by $2J$ and π.

tively, are speculative. A definite determination of these J^π values would be of interest.

^{45}Ca. The best agreement with the predictions and with the fusion-evaporation reaction mechanism is obtained if we choose the 3556-keV level from the two choices offered (Fig. 8) and explain the 3556- and 3942-keV levels as arising from non-normal parity yrast states as indicated in Fig. 12.

^{47}Sc. The predictions give a remarkably consistent picture of this nucleus. Here as in other odd-A $f_{7/2}$ nuclei the non-normal spin sequences suggest a rather simple band structure, as has been noted numerous times in the past.

^{47}Ti. As anticipated, the predictions give a reasonable explanation of the levels to the left in Fig. 1. In addition the 2668-keV level is best explained as a $\frac{9}{2}^+$ level.

^{48}Ti. The speculated odd-parity yrast states are those chosen by Glatz *et al.*[4] from the various possibilities available from their study. We also would choose these levels on the basis of the present calculation.

C. Higher-lying yrast states

One very obvious aspect of the experimental yrast spectra of $f_{7/2}$ shell nuclei is the paucity of normal-parity levels with spins higher than that which can be generated by $(f_{7/2})^n$. For instance, for none of the nuclei considered in

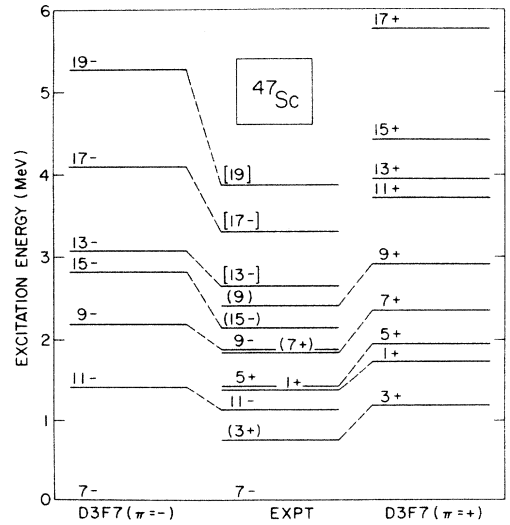

FIG. 13. Experimental and predicted yrast spectra of ^{47}Sc. See the caption of Fig. 11. Note that the levels are labeled by $2J$ and π.

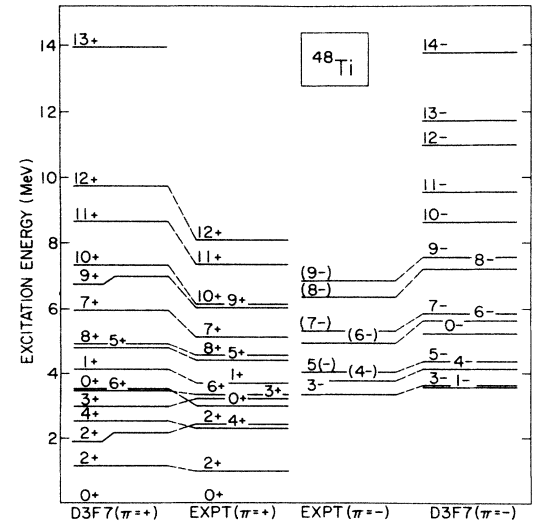

FIG. 15. Experimental and predicted yrast spectra of ^{48}Ti. See the caption of Fig. 11.

TABLE VII. The maximum J^π allowed for the $f_{7/2}^n$ and $(f_{7/2},p_{3/2},f_{5/2},p_{1/2})$ configurational spaces.

Nucleus	J^π_{max} $f_{7/2}^{A-40}$	$(fp)^{A-40}$
^{44}Ca	8^+	10^+
^{45}Ca	$\frac{15}{2}^-$	$\frac{23}{2}^-$
^{47}Ca	$\frac{19}{2}^-$	$\frac{33}{2}^-$
^{47}Ti	$\frac{27}{2}^-$	$\frac{35}{2}^-$
^{48}Ti	12^+	19^+

this report are any such levels identified. (Although some possibilities exist.) The maximum J possible for the full fp shell is shown in Table VII. Our naive expectation would be to observe fp-shell nuclei with higher J values than for the pure $f_{7/2}$ shell and, in some cases, multiparticle-hole states from the excitation of nucleons out of the (s,d) shell. To address this subject we have performed shell-model calculations in the model space

$$[(f_{7/2})^{A-40-n}(p_{3/2},f_{5/2},p_{1/2})^n;\ n=0,1,\ldots,m]\ , \qquad (1)$$

and using the effective interaction of van Hees and Glaudemans[27] as modified for use in $A=48$ by Anderson *et al.*[28,29] We used an unrestricted (fp) space for all nuclei but ^{48}Ti where a restriction to $m=2$ was made.

Relative excitation energies are listed in Table VIII for the two next yrast levels above the maximum spin allowed (J_{max}) for the pure $f_{7/2}$ shell (see Table VII). In this table $E_x(J_{max})$ is the excitation energy calculated for the yrast state with $J=J_{max}$. Results of the $d_{3/2}f_{7/2}$ calculation described in subsection B are also included.

Several observations are immediately evident. (1) Normal parity, i.e., $\pi=(-)^A$, levels of the same J from the fp and $d_{3/2}f_{7/2}$ spaces are close lying; thus, a configurational space including at least parts of both the sd and fp shells would be needed to explore the structure of these states in detail. (2) The $d_{3/2}f_{7/2}$ yrast states of non-normal parity and with $J>J_{max}$ are predicted to lie lower in energy than the $d_{3/2}f_{7/2}$ normal parity states. In most cases they are also predicted to lie lower than the fp yrast states. (3) Finally, and to the point of the present discussion, the energy gaps are large compared to the yrast level separations for $J<J_{max}$. Even if these energy gaps have no influence on the cross section for formation of states with $J>J_{max}$, the large energy gaps mean lower detection efficiency because of than higher energy (efficiency $\sim E_\gamma^{-1}$) and the likelihood of Doppler broadening.

We are interested in obtaining as quantitative an idea as possible of the influence of these energy gaps on the cross section for formation of states with $J<J_{max}$. To address this question we have performed CASCADE (Ref. 9) calculations for ^{47}Ti with the default energy spectrum supplied by the program (see Ref. 9), and also with the level spectrum calculated for the $d_{3/2}f_{7/2}$ space ($0\hbar\omega$–$4\hbar\omega$) as

TABLE VIII. Relative excitation energies (in MeV) calculated for states with $J=J_{max}+1$ and $J_{max}+2$.

Nucleus	J	$E_x(J)-E_x(J_{max})$ fp $\pi=(-)^A$	$d_{3/2}f_{7/2}$ $\pi=(-)^A$	$d_{3/2}f_{7/2}$ $\pi=(-)^{A-1}$
^{44}Ca	9	3.185	2.884	1.546
	10	8.506	3.119	2.878
^{45}Ca	$\frac{17}{2}$	3.830	2.852	2.104
	$\frac{19}{2}$	4.478	3.535	3.096
^{47}Sc	$\frac{21}{2}$	2.424	3.442	2.830
	$\frac{23}{2}$	3.853	4.513	3.740
^{47}Ti	$\frac{29}{2}$	2.997	3.041	1.932
	$\frac{31}{2}$	3.276	4.785	4.675
^{48}Ti	13	1.968	4.218	1.979
	14	3.831	4.943	4.052

described in Sec. III B. In both cases the calculated relative cross section into a particular yrast state was found to be in rough ($\sim$factor of 2) agreement with our experimental results (Table II). For example, in the units of Table II, I_γ for the $\frac{27}{2}^-\rightarrow\frac{23}{2}^-$ and $\frac{23}{2}^-\rightarrow\frac{21}{2}^-$ transitions are predicted (using the default energy spectrum) to be 1140 and 6750, as opposed to the experimental values of 1400(200) and 5730(860); while I_γ for the decay of the unobserved $\frac{29}{2}^-$ state is predicted to be 180 which is below the threshold for observation of any γ transition (see Tables II–V), never mind one predicted to be of $\sim$2 MeV. However, we were surprised to find that this rapid falloff in cross section is due at least as much to the increase in angular momentum as to the energy gap of $\sim$2 MeV between $\frac{27}{2}^-$ and $\frac{29}{2}^-$. Indeed, CASCADE predicts that at $E(^{14}C)=43$ MeV (rather than 34 MeV where our study was made) yields should be observable up to $J\sim\frac{33}{2}$.

IV. SUMMARY

A perusal of the literature shows that—granting probable assignments—the $(f_{7/2})^n$ yrast states and their γ decays are known for all the Ca isotopes. For Sc, unobserved yrast levels occur in ^{46}Sc and no γ decay has been observed for $J^\pi\geq 7^+$ in ^{46}Sc or ^{48}Sc.[30] For Ti, there are missing $(f_{7/2})^n$ yrast states in $A=45$, 46, and 49 and missing γ decays in these nuclei as well as in ^{43}Ti. Thus, the catalog of $(f_{7/2})^n$ levels and their properties in the lower $f_{7/2}$ shell is not complete. Nevertheless, a considerable body of information does exist.

The present study has extended the yrast spectra in ^{45}Ca, ^{47}Sc, and ^{47}Ti and added spectroscopic information in ^{44}Ca and ^{48}Ti. Several directions for further study of these nuclei are indicated. In many the low-spin non-normal parity levels are not definitely established. In ^{44}Ca an interesting $5^\pm$ doublet separated by only 9 keV is possi-

ble with rather unusual γ-decay properties. In all these nuclei, determination of parities—for instance by γ-ray linear polarization measurements—would be of great spectroscopic value. More γ-ray lifetime measurements are needed for a detailed understanding of these yrast spectra. Of great importance for future experimental studies is the prediction from CASCADE that states with spins at least several units higher than possible from $(f_{7/2})^n$ could be observed at $^{14}C+^{36}S$ energies above the $E(^{14}C)=34$ MeV used in the present study.

The shell-model calculations successfully explain the experimental spectra. The success of the $d_{3/2}f_{7/2}$ interaction of Wildenthal is noteworthy. The general feature of too expanded an energy scale could perhaps be rather easily corrected. However, our comparison of (fp) and $d_{3/2}f_{7/2}$ calculations indicates the need for a more expanded configuration space. With present day shell-model codes like OXBASH, it is now possible to calculate in a dfp, or even $sdfp$, space as long as some restrictions are placed on the number of particles in some subshells. Such calculations would appear necessary to explain $E1$ and $M1$ transitions—at least those connecting nonyrast states, Gamow-Teller matrix elements, and almost all structure information for nonyrast states.

ACKNOWLEDGMENTS

We would like to thank B. A. Brown for his instructions in the use of OXBASH, B. H. Wildenthal who very kindly provided us with his $d_{3/2}f_{7/2}$ interaction, and T. W. Burrows for discussions concerning the $A=47$ results. Research supported at Brookhaven National Laboratory under auspices of the U.S. Department of Energy, Division of Basic Energy Sciences, under Contract No. DE-AC02-76CH00016 and at Lawrence Livermore National Laboratory under Contract No. W-7405-ENG-48. The research at SUNY-Stony Brook was supported by the National Science Foundation.

[1]J. D. McCullen, B. F. Bayman, and L. Zamick, Phys. Rev. **134B**, 515 (1964).
[2]W. Kutschera, B. A. Brown, and K. Ogawa, Riv. Nuovo Cimento **1**, No. 12, 1 (1978).
[3]C. Signorini, M. Morando, G. Fortuna, and A. M. Stefanani, in *Proceedings of the EPS International Conference Nuclear Division, Florence, 1977,* edited by P. Blasi and R. A. Ricci (Editrice Compository, Bologna, Italy, 1978), p. 198.
[4]F. Glatz, P. Betz, E. Bitterwolf, A. Burkand, F. Heidinger, Th. Kern. R. Lehman, S. Norbet, and H. Röpke, Z. Phys. A **293**, 57 (1979).
[5]T. Burrows, Nucl. Data Sheets **48**, 1 (1986).
[6]Z. P. Sawa, J. Blomqvist, and W. Guillholmer, Nucl. Phys. **A205**, 257 (1973).
[7]L. Meyer-Schützmeister, G. Hardie, and T. Sjoreen, Phys. Rev. C **14**, 109 (1976).
[8]G. Fortuna, S. Lunardi, M. Morando, and C. Signorini, Nucl. Phys. **A299**, 479 (1978).
[9]F. Puhlhofer, Nucl. Phys. **A280**, 267 (1977).
[10]C. E. Thorn, J. W. Olness, E. K. Warburton, and S. Raman, Phys. Rev. C **30**, 1442 (1984).
[11]E. K. Warburton, J. W. Olness, C. J. Lister, R. W. Zurmühle, and J. A. Becker, Phys. Rev. C **31**, 1184 (1985).
[12]H. J. Rose and D. M. Brink, Rev. Mod. Phys. **39**, 306 (1967).
[13]P. M. Endt, At. Data Nucl. Data Tables **23**, 3 (1979).
[14]M. Toulemonde, L. Deschenes, A. Jarnshidi, and N. Schulz, Nucl. Phys. **A227**, 309 (1974).
[15]P. M. Endt and C. van der Leun, Nucl. Phys. **A310**, 1 (1978).
[16]R. A. Meyer, Lawrence Livermore National Laboratory Report No. M-100, 1978.
[17]E. K. Warburton, J. J. Kolata, J. W. Olness, A. R. Poletti, and Ph. Gorodetzky, At. Data Nucl. Data Tables **14**, 147 (1974).
[18]J. W. Olness, A. H. Lumpkin, J. J. Kolata, E. K. Warburton, J. S. Kim, and Y. K. Lee, Phys. Rev. C **11**, 110 (1975).
[19]D. H. White and R. E. Burkett, Phys. Rev. C **5**, 513 (1972).
[20]H. J. Kim, R. L. Robinson, and W. T. Milner, Phys. Rev. C **11**, 2108 (1975).
[21]H. Nann, D. Mueller, and E. Kashy, Phys. Rev. C **14**, 2089 (1976).
[22]G. Fortuna, R. B. Huber, W. Kutschera, M. Morando, H. Moringa, R. A. Ricci, and C. Signorini, Nuovo Cimento **34A**, 321 (1976).
[23]B. H. Wildenthal, private communication.
[24]B. A. Brown, A. Etchegoyen, W. D. M. Rae, and N. S. Godwin, OXBASH, the Oxford–Buenos Aires Shell Model Code, Cyclotron Laboratory, Michigan State University Internal Report, 1984 (unpublished).
[25]T. Burrows, Nucl. Data Sheets **40**, 149 (1983).
[26]D. E. Alburger, Nucl. Data Sheets **45**, 557 (1985).
[27]A. G. M. van Hees and P. W. M. Glaudemans, Z. Phys. **303**, 267 (1980).
[28]B. D. Anderson, T. Chittrakran, A. R. Baldwin, C. Lebo, R. Madey, P. C. Tandy, J. W. Watson, B. A. Brown, and C. C. Foster, Phys. Rev. C **31**, 1161 (1985).
[29]The parameters of the interaction described in Ref. 28 were determined from a least squares fit to binding energies in the $A\sim51-55$ region using the model space of Eq. (1) with $m=1$. For $m>1$ the extra two-body matrix elements not provided by Ref. 27 were generated from the modified surface delta interaction using the parameters $(A_1,A_0,B_1,B_0)=(0.25, 0.53, -1.09, 0.50)$ MeV.
[30]As shown in Table I, ^{48}Sc was formed in the present study. The expected decay of the known 7_1^+ level was searched for but not found.